Progress In Electromagnetics Research Letter, Vol. 114, 69-74, 2023 PIER Letters

(Received 19 September 2023, Accepted 20 November 2023, Scheduled 27 November 2023)

An Arduino-Controlled Reconfigurable Intelligent Surface with Angular Stability for 5G mmWave Applications

Badisa Anil Babu*, Pulletikurthi Ram Kalyan, Varanasi Venkata Lakhmi, Rana Reharika, and Nakka Varun Raj

Department of ECE, GMR Institute of Technology, Rajam, Vizianagaram 532127, India

ABSTRACT: The role and applications of millimeter wave (mmWave) Reconfigurable Intelligent Surfaces (RIS) have been rapidly increasing by extending the signal coverage with energy and spectrum efficiency. However, the current RIS designs pose challenges like size and angular insensitivity with efficient beamforming functionalities. In this article, we propose a compact and angularly stable RIS unitcell with incident and polarization angle insensitivity in reflection mode. The footprint of the FR4 substrate is $10 \times 10 \times 1.6\,\text{mm}^3$ in size. The unitcell structure consists of circular patch inner cuts as a top layer with a full ground. An AlGaAs pin diode is inserted in the middle of the top layer to get the beamforming. The switchable states provide peak resonance at 32.5 GHz (Bandwidth-444 MHz) and 33.6 GHz (Bandwidth-498 MHz) frequencies. Significant gain values of 11.5 and 13.7 dBi are achieved at the operating frequencies. The designed unitcell provides angular stability up to 90° oblique incidences and polarization angles. The AlGaAs pin diode is controlled by applying suitable bias levels using Arduino Uno. The numerical simulation results and experimental validation are performed with incident and polarization angles, which are suitable for adapting to the challenges in mmWave applications.

1. INTRODUCTION

Reconfigurable Intelligent Surface (RIS) has become the buzzword in recent years due to its spectral and energy efficiency advantage for futuristic mmWave communication applications. RIS can be applied to massive MIMO (Multiple Input Multiple Output) system and mmWave communications in 5G that provide enlarged signal coverage and network scalability [1]. RIS hardware provides benefits like low cost and low power consumption with an increase in system capacity for the current wireless infrastructure [2]. mmWave band provides a high data rate and bandwidth which is crucial for the demand of wireless communication [3]. RIS surfaces have been applied to the mmWave communication infrastructure that provides a smart EM wave propagation environment. Beamforming, beam steering polarization conversion, etc. are key operations obtained using RIS for getting control over the incident EM waves [4].

RIS structures consist of reconfigurable elements to realize intelligent characteristics of the reflected wave. The literature related to RIS surface is updated with the realization of RIS surface hardware focusing on reconfiguration mechanism and application function realization. Most of the RIS literature is realized using electronic switches such as PIN (Positive Intrinsic Negative), Varactor, and Liquid Crystals [5], which was realized for mmWave applications. The most recent literature focused on realizing RIS surfaces with multifunctional, polarization, and incident angle-independent characteristics. The design of polarization and angle insensitive, i.e., angular stable, RIS surface is a challenging task for current mmWave communications [6, 7]. Most of the existing mmWave RIS surfaces have not focused on angle insensitivity which is crucial for mmWave wireless communications.

Furthermore, the research direction tends towards potential programmable RIS surfaces to achieve the real-time characteristics of such beamforming, beam steering, and beam focusing characteristics. Programmability features can be applied to the RIS surfaces by controlling the switching states of the active elements [8–11]. Hence, the programmability for RIS enables the emerging scope in the programmable RIS design. The programmable RIS surface characteristics are realized using embedded boards like FPGA, Arduino, Raspberry Pi, etc. [12–15]. The programmability feature using Arduino for the RIS surface with its operation is illustrated using Fig. 1.

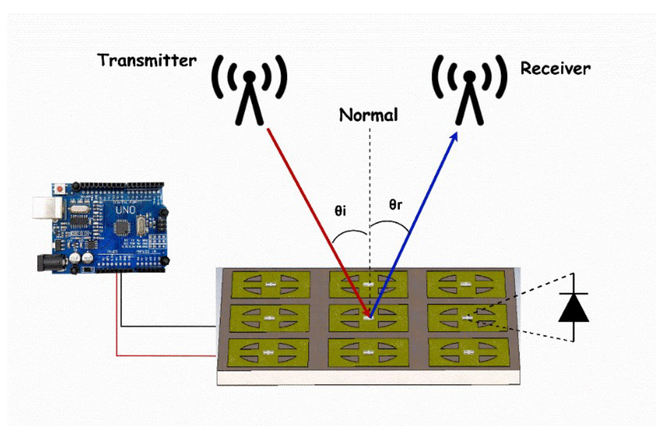

FIGURE 1. Illustration of Arduino-controlled RIS operation.

In this article, an angle and polarization-insensitive compact RIS unitcell operating at mmWave frequencies is realized us-

* Corresponding author: Badisa Anil Babu (anilbabu.b@gmrit.edu.in).

ing an Arduino-controlled AlGaAs PIN diode for beamforming. The unitcell is realized using an FR4 substrate with a footprint of $10 \times 10 \times 1.6\,\text{mm}^3$. The AlGaAs PIN diode is preferred due to its performance at mmWave frequencies. The unitcell design consists of a rectangular patch with symmetric sector cuttings with an AlGaAs PIN diode inserted in the middle. The beamforming characteristics are explained using simulation results by substituting the equivalent diode characteristics of the PIN diode. The biasing circuit is realized using an Arduino board, making the programmability feature for the RIS design. Due to angle insensitive and programmability features, the realized RIS unitcell is suitable for mmWave communications.

2. UNIT CELL DESIGN

The proposed RIS unitcell structure with dimensions is presented in Fig. 2. The design consists of a rectangular metal patch with four symmetric circle sector cuttings and a full ground plane. An FR4 substrate (dielectric constant of 4.4 and loss tangent of 0.025) is used with a footprint of $10 \times 10 \times 1.6\,\text{mm}^3$. In the middle of the patch layer, an AlGaAs pin diode is inserted to get the structure reconfiguration. The equivalent circuit of AlGaAs pin diode (MACOM: MADP-000907-1402P) is used for the design simulation in CST microwave studio as shown in Fig. 3.

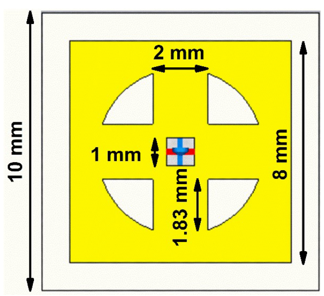

FIGURE 2. Proposed unitcell geometry.

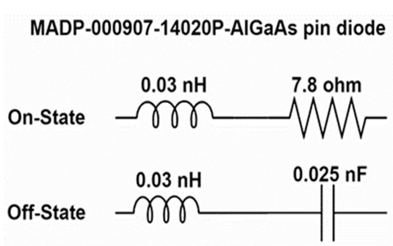

FIGURE 3. Equivalent circuit of AlGaAs diode in bistate [9].

The reflection characteristics of the proposed unitcell are explained using the CST simulation results. In the simulation setup, a linearly polarized wave is incident on the patch layer in a normal direction based on the operating states of the PIN diode with incident and polarization angle changes. The reflection and beamforming behavior of the proposed unitcell is presented in the next section.

3. SIMULATION RESULTS AND REFLECTION CHARACTERISTICS ANALYSIS

The proposed unitcell's reflection characteristics are analyzed using CST Microwave studio tool simulation results. The structure provides dual resonances at 32.5 GHz, and 33.6 GHz peak frequencies with a bandwidth of 444 and 498 MHz, respectively. Fig. 4 shows the reflection coefficient magnitude under the normal incidence of the plane wave.

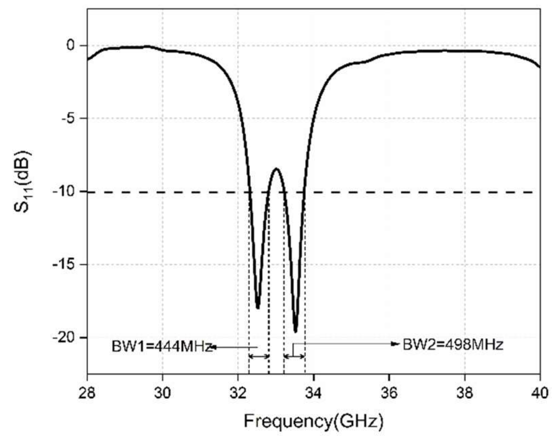

FIGURE 4. Simulated reflection magnitude characteristics of the unitcell.

The reflection magnitude and phase of the unitcell in the on-state is presented in Fig. 5. It is observed that in the on-state, it provides dual resonances with a reflection phase of 0°. Similarly, the off-state reflection characteristics are plotted in Fig. 6. It is observed that the resonance frequency is constant in both operating states except for the resonant peak magnitude value. These simulation results are obtained at both theta and phi $= 0°$, i.e., normal incidence. The reflection characteristics under oblique incidence are constant which is discussed in the below section.

The surface current density of the design at both the resonating frequencies is presented in Fig. 7. In the on-state, the maximum current distribution is located near AlGaAs location in the single-layered structure, whereas the low magnitude of surface current is concentrated in the off state. The resonance behavior is also demonstrated using surface current distribution along the structure.

The beamforming capability of the proposed unitcell is demonstrated using the 3D simulation results as shown in Fig. 8. The peak gain of the unitcell changes in both the operating states at dual frequencies with changes in the beam directions. At 32.5 GHz frequency, it provides a peak gain of 11.5 and 13.7 dBi respectively. Similarly, it provides peak gain values of 12.5 and 13 dBi in the two reconfigurable states.

The angular stability of the proposed unitcell under incident (theta) and polarization (Phi) angles is demonstrated using the simulation results as shown in Fig. 9. Fig. 9 shows the reflection magnitude variations concerning incident and polarization angles. In the reconfigurable states at dual frequencies, the reflection magnitude is stable up to 90°.

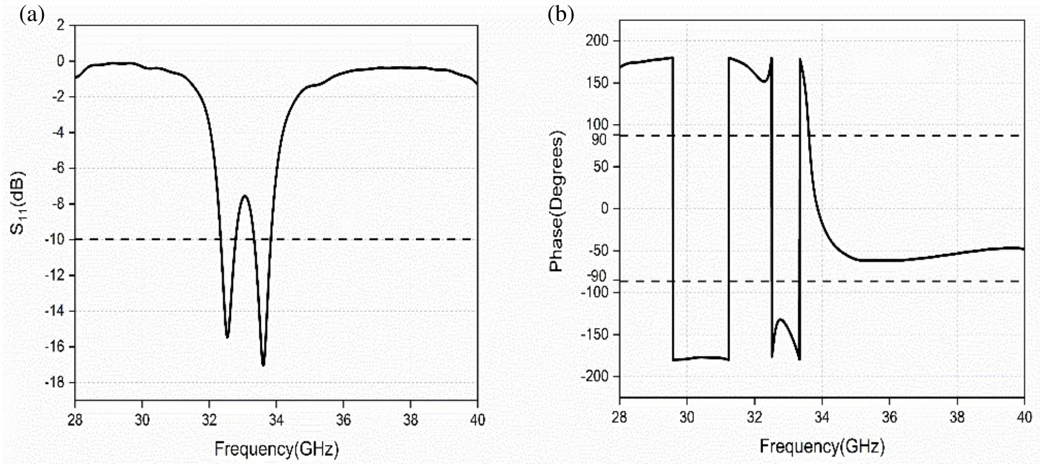

FIGURE 5. Reflection characteristics in on-state. (a) Magnitude. (b) Phase.

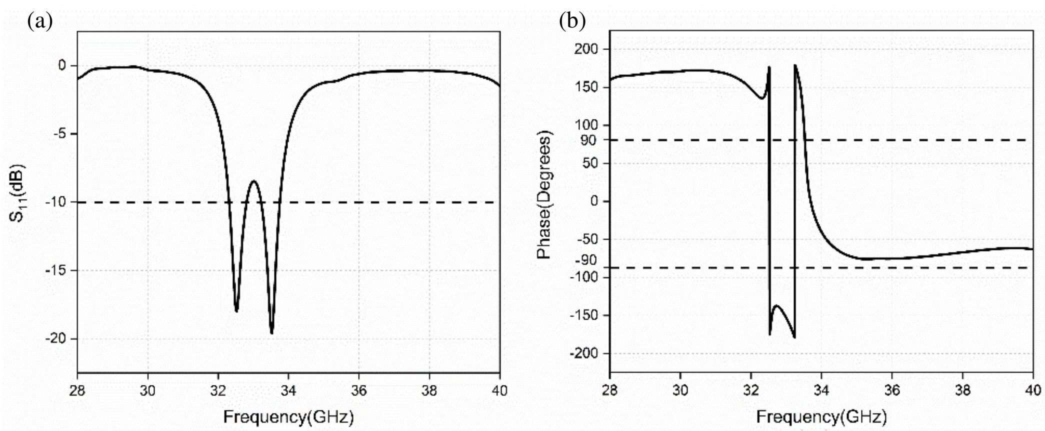

FIGURE 6. Reflection characteristics in off-state. (a) Magnitude. (b) Phase.

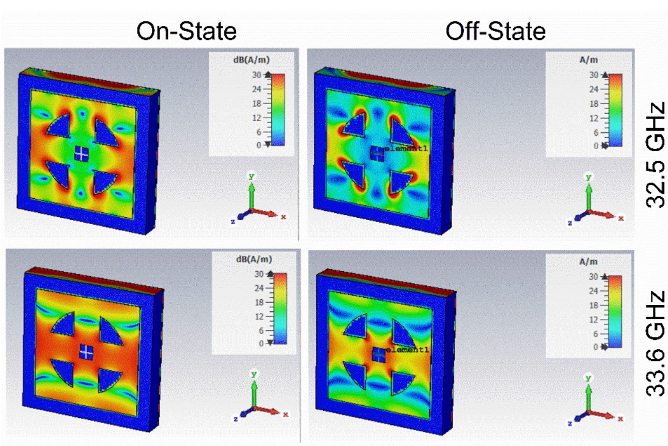

FIGURE 7. Surface current distribution in bistate operation at normal incidence.

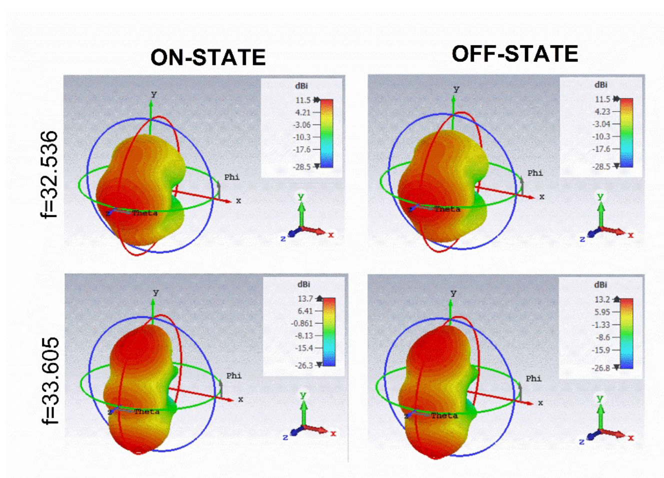

FIGURE 8. Simulated 3D patterns with beamforming capability in reconfigurable states.

4. ARDUINO-BASED BIAS CIRCUIT AND DISCUSSIONS

The programmability for the RIS surface is added using an Arduino board that provides bias control to the AlGaAs PIN diode as shown in Fig. 10. The reconfigurable states are obtained using 1.8 V for on-state and 0 V for off-state. Arduino board provides a cost-effective solution to add the programmability fea-

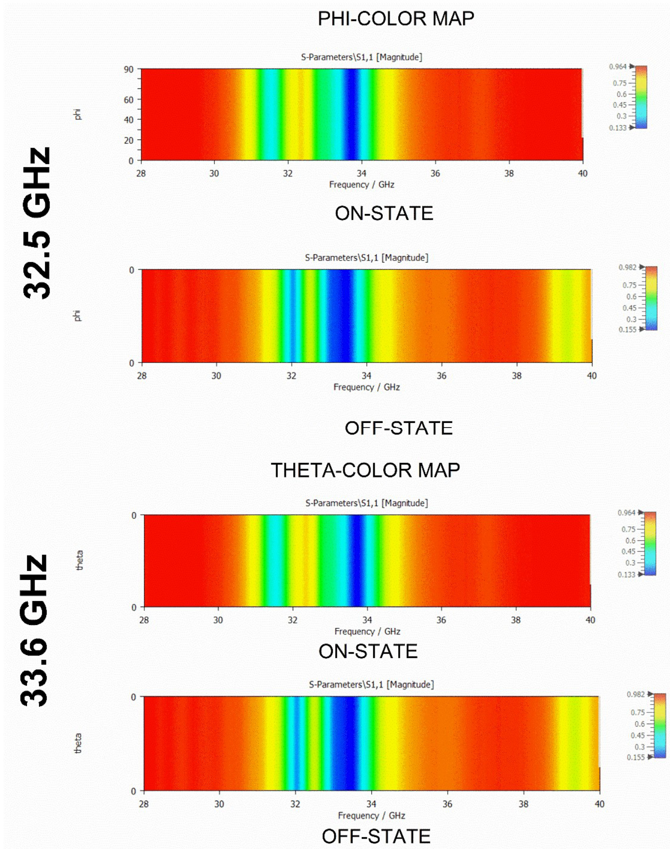

FIGURE 9. Magnitude of reflection characteristics showing angular stability.

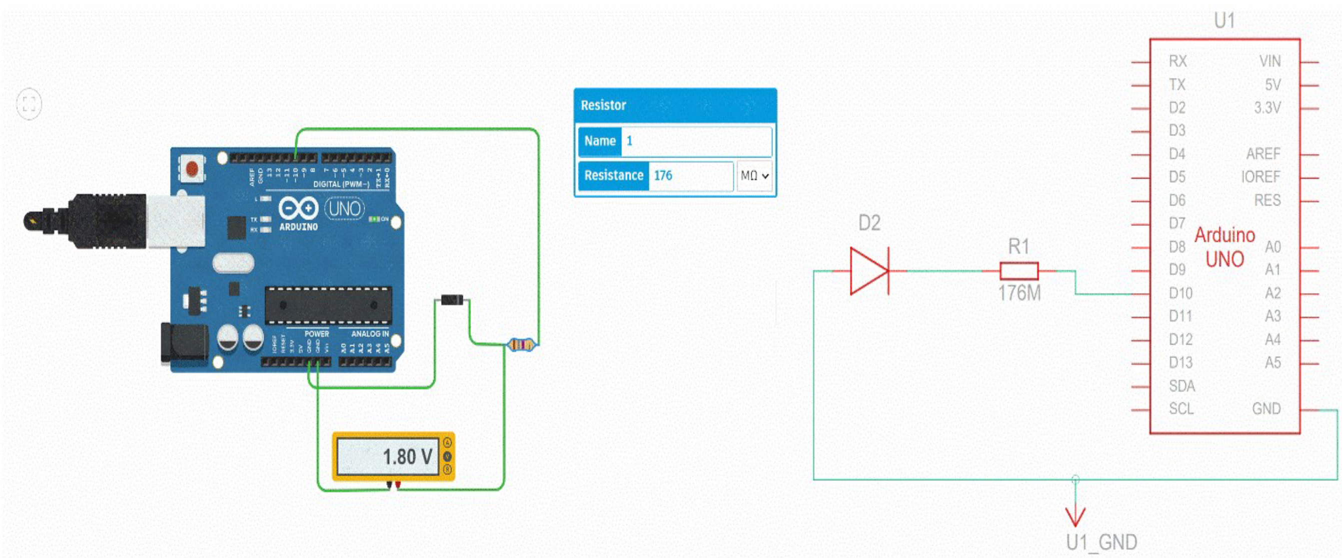

FIGURE 10. AlGaAs diode bias model setup with circuit diagram.

ture using PIN diode bias control for RIS design. The circuit diagram is also shown in Fig. 10.

The effectiveness of the proposed work is analyzed using the existing literature as shown in Table 1. Most of the reported works are focused on manual bias control that limits the optimal design of mmWave RIS. The performance is compared in terms of size and functionality reconfiguration elements. The features of the design with a low profile, angular stability, programmability feature, and reconfiguration mechanism using Arduino board make it a choice for the current demand of mmWave RIS designs.

The fabricated design is shown in Fig. 11. The prototype is fabricated using a CNC PCB printing machine on a commercially available FR4 substrate with pin diodes (MACOM:

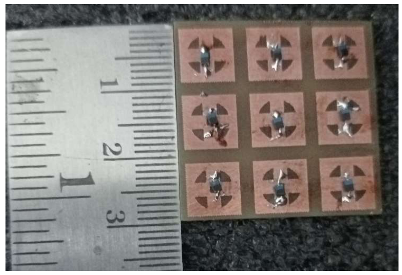

FIGURE 11. Fabricated prototype of 3×3 array size.

TABLE 1. Comparison with existing mmWave RIS surfaces.

Ref.	Unit cell size/ No. of Layers	Frequency (GHz)	No & Diode Type	Functionality/ Programmable device
[8]	$9.5 \times 9.5/2$	28.5	1 & PIN	Beamforming/Control board using FPC connectors
[9]	$7.1 \times 7.1/2$	27.5	1 & AlGaAs pin	Beam steering/Voltage control
[10]	$16 \times 16/3$	28.5	5 & PIN	Beamforming/FPGA
[11]	$4.3 \times 8.6/1$	28.5	2 & PIN	Beamforming/FPGA
Proposed	$10 \times 10/1$	32.5 & 33.6	1 & AlGaAs	Beamforming/Arduino

* FPGA — Field Programmable Gate Array

MADP-000907-1402P). The Arduino-based bias setup is added to the prototype that enables programmability features to RIS design.

5. CONCLUSION

In this work, we synthesize an Arduino-controlled mmWave RIS unitcell design that offers angular stability and beamforming capability for 5G mm-wave communications. The design is realized using an AlGaAs PIN diode suitable at mmWave frequencies and resonates at 32.5 and 33.6 GHz frequencies. The reflection characteristics are polarization and incident angle insensitive, providing angular stability up to 90°. These characteristics are analyzed using the CST numerical simulation results. The design is converted into a programmable RIS design by providing Arduino-based bias control. The design methodology along with the functional characterization is also discussed. Hence, the proposed Arduino-controlled RIS surface has the potential to satisfy the demand of futuristic 5G mmWave communication applications.

REFERENCES

[1] Liu, Y., X. Liu, X. Mu, T. Hou, J. Xu, M. Di Renzo, and N. Al-Dhahir, "Reconfigurable intelligent surfaces: Principles and opportunities," *IEEE Communications Surveys and Tutorials*, Vol. 23, No. 3, 1546–1577, 2021.

[2] Pan, C., H. Ren, K. Wang, J. F. Kolb, M. Elkashlan, M. Chen, M. Di Renzo, Y. Hao, J. Wang, A. L. Swindlehurst, X. You, and L. Hanzo, "Reconfigurable intelligent surfaces for 6G systems: Principles, applications, and research directions," *IEEE Communications Magazine*, Vol. 59, No. 6, 14–20, Jun. 2021.

[3] Rappaport, T. S., Y. Xing, G. R. MacCartney, Jr., A. F. Molisch, E. Mellios, and J. Zhang, "Overview of millimeter wave communications for fifth-generation (5G) wireless networks-with a focus on propagation models," *IEEE Transactions on Antennas and Propagation*, Vol. 65, No. 12, 1, 6213–6230, Dec. 2017.

[4] Rana, B., S.-S. Cho, and I.-P. Hong, "Review paper on hardware of reconfigurable intelligent surfaces," *IEEE Access*, Vol. 11, 29 614–29 634, 2023.

[5] Saifullah, Y., Y. He, A. Boag, G.-M. Yang, and F. Xu, "Recent progress in reconfigurable and intelligent metasurfaces: A comprehensive review of tuning mechanisms, hardware designs, and applications," *Advanced Science*, Vol. 9, No. 33, 1–35, Nov. 2022.

[6] Zhang, L. and T. J. Cui, "Angle-insensitive 2-bit programmable coding metasurface with wide incident angles," in *Proceedings of The 2019 IEEE Asia-Pacific Microwave Conference (APMC)*, 932–934, Singapore, Dec. 2019.

[7] Liang, J. C., Q. Cheng, Y. Gao, C. Xiao, S. Gao, L. Zhang, S. Jin, and T. J. Cui, "An angle-insensitive 3-bit reconfigurable intelligent surface," *IEEE Transactions on Antennas and Propagation*, Vol. 70, No. 10, 8798–8808, Oct. 2022.

[8] Wang, R., Y. Yang, B. Makki, and A. Shamim, "A wideband reconfigurable intelligent surface for 5G millimeter-wave applications," *Arxiv Preprint Arxiv: 2304.11572*, 2023.

[9] Shekhawat, A. S., B. G. Kashyap, P. C. Theofanopoulos, A. P. S. Sengar, and G. C. Trichopoulos, "A compact unit-cell design for mmWave reconfigurable intelligent surfaces," in *2022 United States National Committee of URSI National Radio Science Meeting (USNC-URSI NRSM)*, 84–85, Boulder, CO, USA, 2022.

[10] Dai, L., B. Wang, M. Wang, X. Yang, J. Tan, S. Bi, S. Xu, F. Yang, Z. Chen, M. Di Renzo, C.-B. Chae, and L. Hanzo, "Reconfigurable intelligent surface-based wireless communications: Antenna design, prototyping, and experimental results," *IEEE Access*, Vol. 8, 45 913–45 923, 2020.

[11] Gros, J.-B., V. Popov, M. A. Odit, V. Lenets, and G. Lerosey, "A reconfigurable intelligent surface at mmWave based on a binary phase tunable metasurface," *IEEE Open Journal of The Communications Society*, Vol. 2, 1055–1064, 2021.

[12] Saifullah, Y., F. Zhang, G.-M. Yang, and F. Xu, "3-bit programmable reflective metasurface," in *2018 12th International Symposium on Antennas, Propagation and Electromagnetic Theory (ISAPE)*, Propagation and Electromagnetic Theory (ISAPE), Hangzhou, Dec. 2018.

[13] Trichopoulos, G. C., P. Theofanopoulos, B. Kashyap, A. Shekhawat, A. Modi, T. Osman, S. Kumar, A. Sengar, A. Chang, and A. Alkhateeb, "Design and evaluation of reconfigurable intelligent surfaces in real-world environment," *IEEE Open Journal of The Communications Society*, Vol. 3, 462–474, 2022.

[14] Hu, J., H. Zhang, B. Di, L. Li, K. Bian, L. Song, Y. Li, Z. Han, and H. V. Poor, "Reconfigurable intelligent surface based RF sensing: Design, optimization, and implementation," *IEEE Journal on Selected Areas in Communications*, Vol. 38, No. 11, 2700–2716, Nov. 2020.

[15] Vamseekrishna, A., B. T. P. Madhav, T. Anilkumar, and L. S. S. Reddy, "An IoT controlled octahedron frequency reconfigurable multiband antenna for microwave sensing applications," *IEEE Sensors Letters*, Vol. 3, No. 10, 1–4, Oct. 2019.